Electronic Supplementary Information (ESI)

Near-infrared phosphorescent iridium(III) complex for imaging of cysteine and homocysteine in living cells and *in vivo*

Yongquan Wu[a], Renmiao Wu[a], Huifang Li[a], Hong Zeng[a], Yuanyan Li[a], Qiuhong Wang[b], Mei Shi*[b] and Xiaolin Fan*[a]

[a] School of Chemistry and Chemical Engineering & Key Laboratory of Organo-pharmaceutical Chemistry of Jiangxi Province, Gannan Normal University, Ganzhou, 341000, P. R. China

[b] Department of Chemistry, Fudan University, Shanghai 200433, P. R. China

Fax: +86-797-8393536, +86-21-55664621. E-mail: fanxl2013@gnnu.cn, shimei@fudan.edu.cn

Experimental section

Materials

All solvents, unless specified, were purchased from Shanghai Titan Scientific Co., Ltd (China), and were used without further purification. 2-chloroquinoline-3-carbaldehyde and benzo[b]thiophen-2-boronic acid were purchased from Energy Chemical Co., Ltd (China). 1,10-phenanthroline, $Pd[P(Ph)_3]_4$, K_2CO_3, and KPF_6 were purchased from Aladdin Technology Co., Ltd (China). $IrCl_3 \cdot 3H_2O$ was purchased from Rock New Material Co., Ltd (China). MTT and PBS were purchased from Beyotime Biotechnology Co., Ltd (China). DMEM, RPMI 1640, and FBS were purchased from Thermo Fisher Scientific Co., Ltd. Alanine (Ala), arginine (Arg), aspartic acid (Asp), glutamine (Gln), glutamic acid (Glu), glycine (Gly), glutathione (GSH), histidine (His), isoleucine (Ile), leucine (Leu), lysine (Lys), methionine (Met), phenylalanine (Phe), proline (Pro), serine (Ser), threonine (Thr), tryptophan (Trp), tyrosine (Tyr) and valine (Val) and Cys were supplied from Aladdin Technology Co., Ltd. N-ethylmaleimide (Adamas) was obtained from Adamas Reagents Co., Ltd (China). Hcy was purchased from Sigma-Aldrich.

General instrument for characterization

^{1}H NMR and ^{13}C NMR spectra were recorded on Bruker DRX-400 NMR spectrometers with tetramethylsilane as the internal standard. Mass spectra were

collected with an AB SCIEX mass spectrometer. The UV-visible spectra were recorded on a Shimadzu UV-2007 spectrometer. Steady-state emission experiments at room temperature were measured on an Edinburgh Instruments spectrometer FS-5. The luminescence quantum yield in air-equilibrated solution were measured with reference to tris-(2,2'-bipyridyl)-ruthenium (II) chloride hexahydrate as a standard (Φ=0.063 in DMF). Lifetime studies were performed with an Edinburgh FL 920 photo-counting system with a hydrogen filled lamp as the excitation source.

Synthesis details

The synthesis routine of ligand **1** and **NIR-Ir** were shown at Scheme S1.

Synthesis of ligand L1. 2-chloroquinoline-3-carbaldehyde (4 mmol) and benzo[b]thiophen-2-boronic acid (4 mmol) were added to a flask, 40 mL mixed solvent of THF and water (1:1, v/v) was added, K_2CO_3 (12 mmol) and terakis (triphenylphosphine) palladium (0) (0.28 mmol) were added then. The mixture was heated to 70 ^{0}C for 24 h under N_2 atmosphere. After it was cooled, the mixture was poured into water and extracted with dichloromethane (20 mL×3). The combined organic phases were dried over anhydrous Na_2SO_4, filtered and evaporated to dryness. The raw product was purified by silica gel chromatograph using CH_2Cl_2/PE as eluent (1:2, v/v). ^{1}H NMR (400 MHz, $CDCl_3$) δ= 10.55 (s, 1H), 8.82 (s, 1H), 8.23 (d, *J* = 8.5 Hz, 1H), 8.01 (d, *J* = 8.0 Hz, 1H), 7.98 – 7.92 (m, 1H), 7.89 (dd, *J* = 7.1, 5.9 Hz, 2H), 7.65 (t, *J* = 7.5 Hz, 1H), 7.60 (s, 1H), 7.49 – 7.40 (m, 2H). ^{13}C NMR (100 MHz, $CDCl_3$) δ 190.94, 153.00, 149.48, 141.36, 141.23, 140.04, 138.58, 132.76, 129.53, 129.36, 127.87, 127.82, 127.69, 126.30, 125.75, 124.78, 124.55, 122.39. MS (MALDI-TOF-MS): calcd for $C_{18}H_{12}NOS$, 290.0640 (M^+), found: 290.60 (M^+).

Synthesis of NIR-Ir. A mixed solvent of 2-ethoxyethanol and water (3:1, v/v) was added to a flask containing $IrCl_3 \cdot 3H_2O$ (0.75 mmol) and **L1** (1.5 mmol). The mixture was refluxed for 24 h, and filtered to obtain the cyclometalated iridium(III) chloro-bridged dimeric intermediate $[Ir(ligand)_2Cl_2]_2$. A mixture of dichloro-bridged dimeric intermediate product (482.6 mg, 0.3 mmol) and 1,10-phenanthroline monohydrate (120.9 mg, 0.60 mmol) in methanol/ dichloromethane (30 mL, v/v=1:2) solution was refluxed at 50 ^{0}C under N_2 atmosphere for 10 h. Potassium hexafluorophosphate

(180.4 mg, 7.5 mmol) was added to the solution with stirring for 4 h. The raw product was purified by silica gel chromatograph using CH_2Cl_2/CH_3OH as eluent (20:1, v/v). ^{1}HNMR (400 MHz, DMSO) δ = 11.00 (s, 2H), 9.06 (d, *J* = 5.0 Hz, 2H), 8.95 (s, 2H), 8.74 (d, *J* = 8.1 Hz, 2H), 8.12 (dd, *J* = 8.2, 5.3 Hz, 2H), 8.06 (d, *J* = 8.1 Hz, 2H), 8.00 (s, 2H), 7.90 (d, *J* = 7.6 Hz, 2H), 7.22 (dd, *J* = 14.9, 7.5Hz, 4H), 7.09 (d, *J* = 8.9 Hz, 2H), 6.92 (t, *J* = 7.4 Hz, 2H), 6.73 (t, *J* = 7.6 Hz, 2H), 6.47 (d, *J* = 8.2 Hz, 2H). ^{13}C NMR (100 MHz, d^6-DMSO) δ 190.08, 165.69, 158.59, 150.37, 150.04, 149.51, 145.97, 145.45, 145.39, 144.70, 140.05, 138.01, 136.67, 133.98, 131.22, 130.33, 128.93, 128.27, 128.01, 127.86, 127.67, 127.36, 127.14, 126.34, 125.31, 124.46, 123.76, 123.61, 123.26. MS (MALDI-TOF-MS): calcd for $C_{48}H_{29}IrN_4O_2S_2$, 950.1165(M^+), found, *m/z* 950.94 (M^+).

Measurement of photophysical properties

UV-visible spectra were recorded on Shimadzu UV-2007 spectrometer and their emission spectra were recorded on Edinburgh FS-5 spectrometer in ethanol solution at room temperature. Lifetime studies were performed with an Edinburgh FL 920 photo-counting system with a hydrogen filled lamp as the excitation source. The data were analyzed by iterative convolution of the luminescence decay profile with the instrument response function using a software package provided by Edinburgh Instruments.

Quantum yields were calculated according to the literature at room temperature.[1] The samples solution was diluted by ethanol, and the aerated DMF solution of tris (2,2'-bipyridyl) ruthenium (II) chloride hexahydrate (0.063 in DMF) was utilized as the reference. The quantum yields of the complexes were calculated according to eq. $\Phi_\mu=\Phi_s I_\mu A_s N_\mu^2/I_s A_\mu N_s^2$. where, 'N' represents the solution's refractive index, 'I' represents the integrated fluorescence intensity, 'A' represents the integrated absorbance intensity, and the subscripts 'μ' and 's' refer to the reference samples and the samples, respectively.

The amino acids titration of NIR-Ir

Spectrophotometric determination was carried out in DMSO-HEPES (pH 7.4, 4:1 v/v) at room temperature. Different concentrations of various amino acids were

titrated into a solution of **NIR-Ir** (10 μM) in DMSO-HEPES, respectively. Before UV-vis absorption and photoluminescence spectra of the samples were measured, the solutions were kept at 37 ^{0}C for 2 hours. For luminescence measurements, excitation was provided at 495 nm, and emission was collected from 600 to 800 nm.

Computational details

These iridium complexes were optimized with density functional theory (DFT)[1] using the Becke's three-parameter hybrid exchange functional combined with the Lee-Yang-Parr correlation functional (B3LYP)[2], a functional that has been widely employed in previous studies of iridium complexes. [3] The "double-ζ" quality basis set LANL2DZ and corresponding effective core potentials[4] were used for iridium atom, while the 6-31G(p,d)[5] basis set was used on nonmetal atoms in the gradient optimizations. All optimized configurations were confirmed to be minima on the potential energy surfaces by performing vibrational frequency calculations at the same level. In addition, a conductor-like polarizable continuum model (CPCM)[6] using ethanol (ε = 24.852) as the solvent was considered for optimization calculations of the involved geometries. Calculations were performed with Gaussian 09 (Revision D.01)[7]. To shed more light on the nature of the excited states of these Ir(III) compounds, vertical transition energies were calculated on the basis of the optimized S_0 and T_1 structures via time-dependent DFT (TDDFT).[89] Natural transition orbital (NTO)[10] analyses were performed further to examine the nature of the excited states.

Cytotoxicity assay

The HeLa cell lines were provided by the Institute of Biochemistry and Cell Biology (Chinese Academy of Sciences). The HeLa cells were grown in DEME (Dulbecco's Modified Eagle Medium) supplemented with 10% FBS (Fetal Bovine Serum) at 37 ^{0}C and 5% CO_2.

In vitro cytotoxicity was measured by performing methyl thiazolyl tetrazolium (MTT) assays on the HeLa cells. Cells were seeded into a 96-well cell culture plate at 5×10^3/well, and were cultured at 37 ^{0}C and 5 % CO_2 for 24 h. Different concentrations of NIR-Ir (0, 5, 10, 15, 20, and 25 μmol/L, diluted in DEME) were then added to the wells. The cells were subsequently incubated for 24 h at 37 ^{0}C under

5% CO_2. Thereafter, MTT (5 mg/mL) was added to each well and the plate was incubated for an additional 5 h at 37 ^{0}C under 5 % CO_2. The optical density OD570 value (Abs.) of each well, with background subtraction at 690 nm, was measured by means of a microplate reader (KHB ST360, China). The following formula was used to calculate the inhibition of cell growth: Cell viability (%) = (mean of Abs. value of treatment group/mean of Abs. value of control) × 100%.

Confocal luminescence imaging

Confocal luminescence imaging of cells was performed with an OLYMPUS FV1000 laser scanning microscope, and a 40 oil-immersion objective lens was used. For fluorescence imaging, MCF-7 cells were incubated on glass bottom dishes for 12 h. Excitation of the MCF-7 cells at 532 nm was carried out with a laser, and emission was collected at 700±50 nm using a PMT detector. Prior to imaging, the medium was removed. Cell imaging was carried out after washing cells with PBS (pH=7, 10 mM) three times.

***In vivo* imaging**

Animal procedures were in agreement with the guidelines of the Institutional Animal Care and Use Committee. *In vivo* luminescence imaging was performed with a modified luminescence *in vivo* imaging system (IVScpoe 7550, Shanghai CLINX Science Instruments Ltd., China). In this system, two external 0 − 5 W adjustable CW 532 nm lasers (Changchun Laser Optoelectronics Technology Ltd., China) and an Andor CCD (IKON-M934BV, Andor Technology Ltd., UK) were used as the excitation sources and the signal collector, respectively. Images of luminescent signals were analyzed with Kodak Molecular Imaging Software. Luminescence signals were collected at > 650 nm with a longpass filter (Semrock, INC).

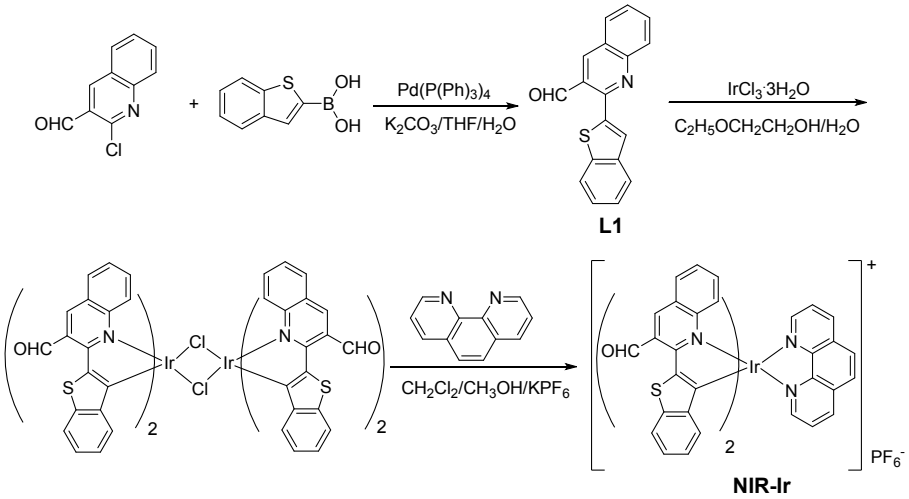

Scheme S1 Synthetic routine of complex **NIR-Ir**

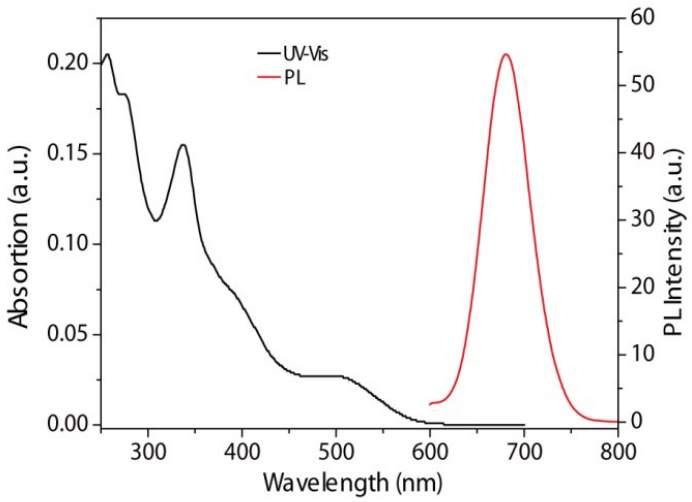

Figure S1. Absorption and emission spectra of **NIR-Ir** in DMSO-HEPES (pH 7.4, 4:1 v/v)

Table S1. Photophysical data of complex NIR-Ir, NIR-Ir+Cys, and NIR-1+Hcy

Complex	Solvent	λ_{abs}/nm (ε/dm^3 mol^{-1} cm^{-1})	$\lambda_{PL,max}$(nm)	Φ_{em}	τ(ns)
NIR-1	CH_3CH_2OH	261(43090), 345(25818), 500 (4818)	680	0.008	158
NIR-1+Cys	CH_3CH_2OH	261(41851), 345(21232), 500 (5038)	670	0.018	-
NIR-1+Hcy	CH_3CH_2OH	261(41212), 345(21554), 500 (5012)	670	0.021	-

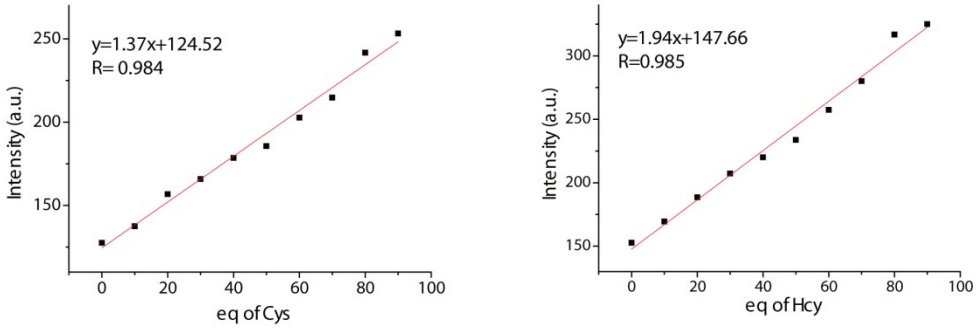

Figure S2. Plots of emission intensity at 684 nm versus various amounts of Cys/Hcy (0-90 equiv) in DMSO-HEPES buffer

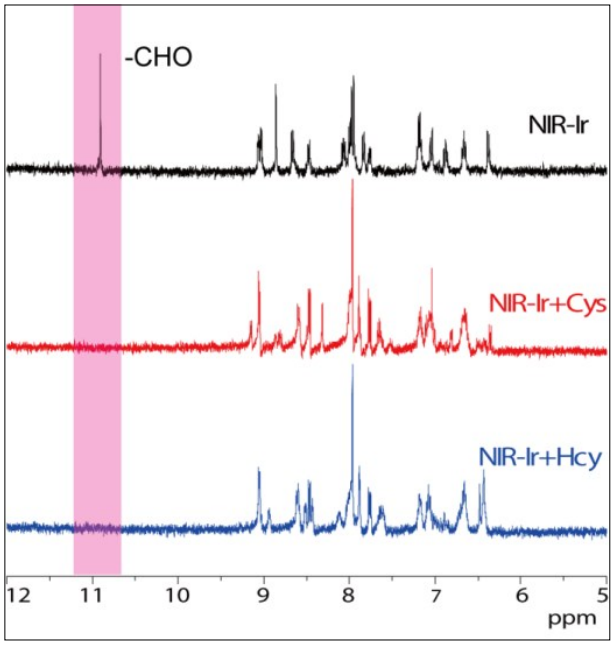

Figure S3. Partial ^{1}H NMR spectral changes of **NIR-Ir** in d^{6}-DMSO in the presence of excess Cys and Hcy

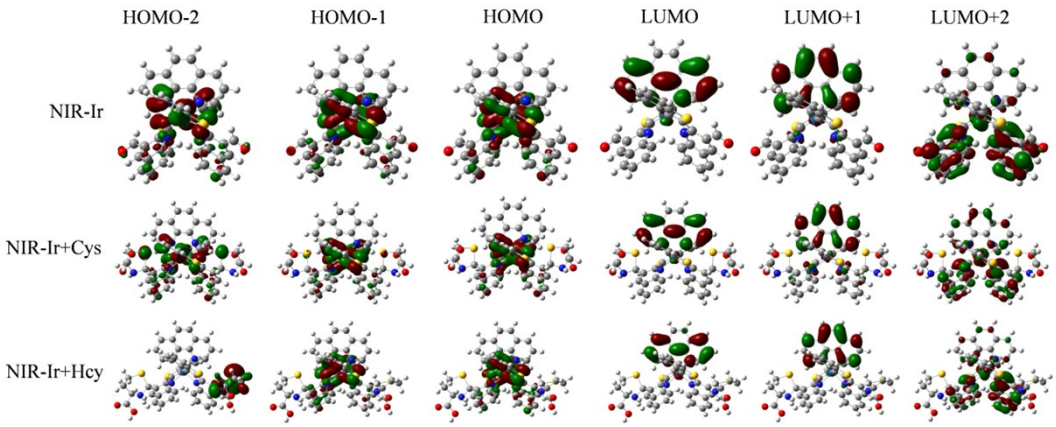

Figure S4. Representations of the frontier molecular orbitals (MOs) for the S_0 geometry of NIR-Ir, NIR-Ir+Cys, and NIR-Ir+Hcy as determined at the B3LYP/[LANL2DZ-ECP/6-31G(d,p)] level of theory

Table S2. Energies for the frontier MOs obtained the B3LYP/[LANL2DZ-ECP/6-31G(d,p)] level. (in eV)

Sample	HOMO-2	HOMO-1	HOMO	LUMO	LUMO+1	LUMO+2	gap
NIR-Ir	-8.78	-8.19	-8.14	-5.14	-5.05	-4.65	3.00
NIR-Ir+Cys	-8.20	-7.59	-7.58	-4.39	-4.33	-4.03	3.19
NIR-Ir+Hcy	-8.19	-7.77	-7.74	-4.70	-4.66	-4.23	3.04

Table S3. Vertical absorption and emission energies (in eV), dominated orbital excitations obtained from TD-DFT calculations. The absorption energies are based on the S_0 state equilibrium geometry.

Sample	S-linked	$\lambda_{abs.}$	f（oscillator strengths）
NIR-Ir	$S_0 \rightarrow S_1$	2.2269 eV 556.76 nm	0.0007
	$S_0 \rightarrow S_2$	2.3028 eV 538.42 nm	0.0025
	$S_0 \rightarrow S_3$	2.4074 eV 515.02 nm	0.0020
	$S_0 \rightarrow S_4$	2.4639 eV 503.20 nm	0.0113
	$S_0 \rightarrow S_5$	2.7668 eV 448.12 nm	0.0306
	$S_0 \rightarrow S_6$	2.7890 eV 444.55 nm	0.0427
	$S_0 \rightarrow S_7$	2.8714 eV 431.79 nm	0.0042
	$S_0 \rightarrow S_8$	2.8714 eV 431.78 nm	0.0150
	$S_0 \rightarrow S_9$	2.9208 eV 424.49 nm	0.0009
	$S_0 \rightarrow S_{10}$	2.9258 eV 423.75 nm	0.0009
NIR-Ir+Cys	$S_0 \rightarrow S_1$	2.4117 eV 514.09 nm	0.0027
	$S_0 \rightarrow S_2$	2.4385 eV 508.44 nm	0.0055
	$S_0 \rightarrow S_3$	2.5466 eV 486.87 nm	0.0104
	$S_0 \rightarrow S_4$	2.5713 eV 482.19 nm	0.0380
	$S_0 \rightarrow S_5$	2.8108 eV 441.10 nm	0.0358
	$S_0 \rightarrow S_6$	2.8332 eV 437.62 nm	0.0907
	$S_0 \rightarrow S_7$	2.8700 eV 432.00 nm	0.0161
	$S_0 \rightarrow S_8$	2.8901 eV 428.99 nm	0.0258
	$S_0 \rightarrow S_9$	3.0988 eV 400.11 nm	0.0063
	$S_0 \rightarrow S_{10}$	3.1028 eV 399.58	0.0008

		nm	
NIR-Ir+Hcy	$S_0 \rightarrow S_1$	2.2107 eV 560.84 nm	0.0007
	$S_0 \rightarrow S_2$	2.2915 eV 541.06 nm	0.0028
	$S_0 \rightarrow S_3$	2.3767 eV 521.66 nm	0.0032
	$S_0 \rightarrow S_4$	2.4390 eV 508.35 nm	0.0155
	$S_0 \rightarrow S_5$	2.7598 eV 449.25 nm	0.0451
	$S_0 \rightarrow S_6$	2.8387 eV 436.76 nm	0.1110
	$S_0 \rightarrow S_7$	2.8616 eV 433.27 nm	0.0178
	$S_0 \rightarrow S_8$	2.8942 eV 428.39 nm	0.0007
	$S_0 \rightarrow S_9$	2.9147 eV 425.38 nm	0.0048
	$S_0 \rightarrow S_{10}$	2.9235 eV 424.09 nm	0.0059

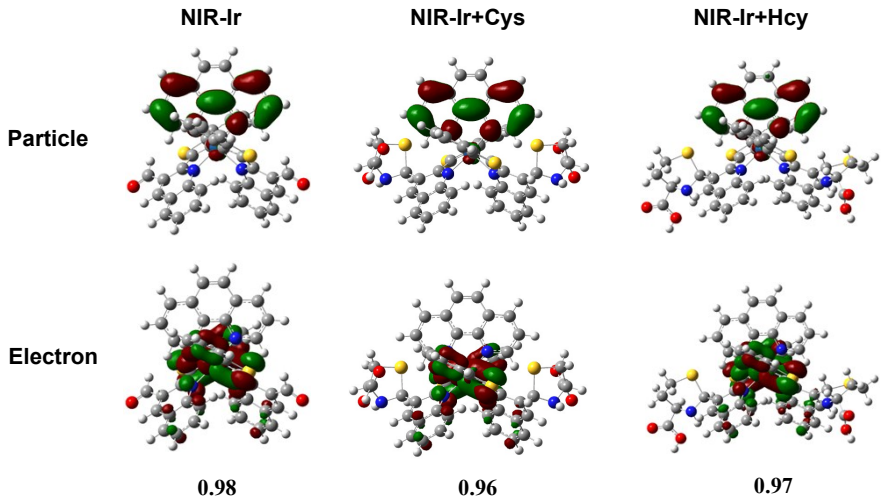

Figure S5. TD-NTO analysis for the dominant pair of the hole-particle wave function pairs of natural transition orbital for the S_1 state based on the optimized geometries in the ground state. The corresponding square of the singular value is denoted on the bottom.

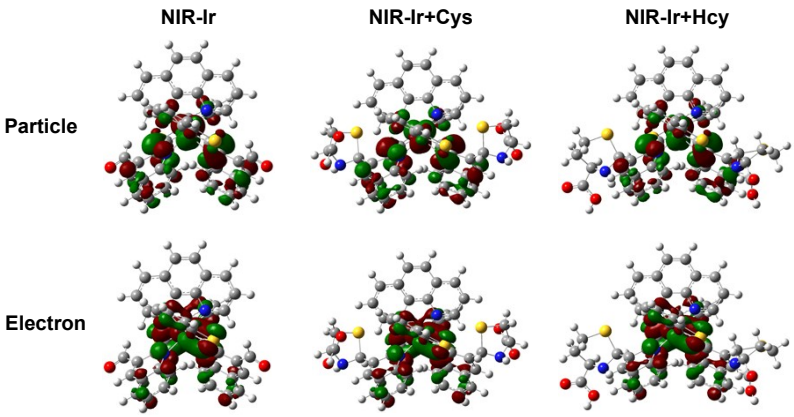

Figure S6. TD-NTO analysis for hole-particle wave function pairs of natural transition orbital for the T_1 state based on the optimized geometries in the triplet state.

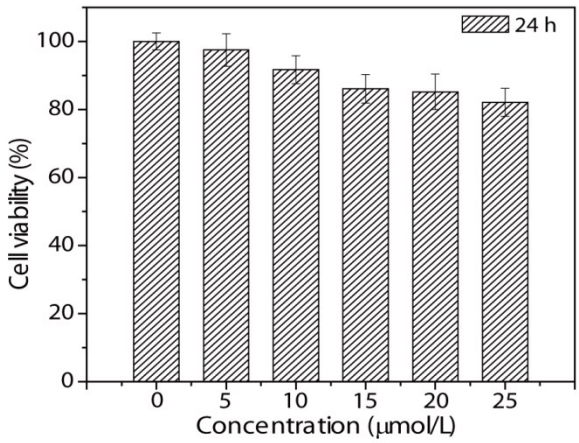

Figure S7. Cell viability values (%) estimated by MTT proliferation test versus incubation concentrations of **NIR-Ir**. HeLa cells were cultured in the presence of 5-25 μM complex **NIR-Ir** at 37 ^{0}C for 24 h

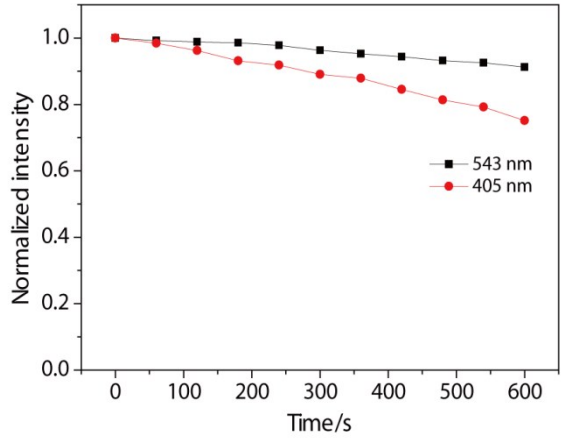

Figure S8. Photobleaching curves of **NIR-Ir** treated cells under excitation at 405 or 543 nm with high power density. The emission signal at 650−750 nm of **NIR-Ir** was collected

Table S4 Comparison of Cys or Hcy imaging with Ir (III) complex probe

Reference	λ_{ex} /nm	$\lambda_{em\ max}$ / nm	Imaging application
This work	543	680	MCF-7 cells
	532	680	BALB/c mouse
Chen et al. *Inorg. Chem.*, 2007, 46, 11075–11081	510	615	Not given
Xiong, et al. *Inorg. Chem.*, 2010, 49, 6402–6408	405	547	KB cells
Ma et al. *J. Mater. Chem.*, 2011, 21, 18974–18982	405	572	KB cells
Shiu et al. *Chem. Commun.*, 2011, 47, 4367–4369	360	590	Not given
Zhao, et al. *Dalton Trans.*, 2010, 39, 8288–8295	350	587	Not given
Cao et al. *J. Mater. Chem.*, 2012, 22, 2650–2657	365	570	Not given
Huang, et al. *Chem. Commun.*, 2012, 48, 11760–11762	370	590	Not given
Liu, et al. *J. Mater. Chem.*, 2012, 22, 7894–7901	405	541	KB cells
Dong, et al. *Luminescence*, 2012, 27, 414–418	-	590	Not given
Li, et al. *Chem. Commun.,* 2013, 49, 2040−2042	405	564	HeLa cells
Liu, et al. *Macromol. Rapid Commun.* 2013*, 34,* 81−86	405	567	KB cells
Ma, et al. *J. Mater. Chem. B*, 2013, 1, 319–329	405	546	KB cells
Tang, et al. *Chem. Eur. J.*, 2013, 19, 1311–1319	405	603	HeLa cells
Chen et al. *Analyst*, 2013, 138, 6742–6745	323	606	Not given
Xu et al. *Adv. Healthcare Mater.*, 2014, 3, 658–669	405/808	650	KB cells
Mao, *et al*. *Chem. Commun.*, 2016, 52, 4450–4453	405	580	Zebrafish
Gao, et al. *Sensors and Actuators B,* 2017, 245, 853–859	405	563	HeLa cells
Kim, et al. *Biosensors and Bioelectronics*, 2017, 91, 497–503	-	655	Not given

References

1. (a) G. A. Crosby and J. N. Demas, *J. Phys. Chem.*, 1971, **75**, 991; (b) J. V. Caspar and T. J. Meyer, *J. Am. Chem. Soc.*, 1983, **105**, 5583.
2. A. D. Becke, *J. Chem. Phys.* 1993, **98**, 5648.
3. (a) C. Lee, W. Yang, R. G. Parr, *Phys. Rev. B,* 1988, **37**, 785. (b) A. D. Becke, *J. Chem. Phys*. 1993, **98**, 5648.
4. (a)H. F. Li, P. Winget, C. Risko, J. S. Sears, J -L. Brédas, *Phys. Chem. Chem. Phys.* 2013, **15**, 6293. (b) J-Y. Hung, C-H. Lin, Y. Chi, M-W. Chung, Y-J. Chen, G-H. Lee, P-T. Chou, C-C. Chen, C-C. Wu, *J. Mater. Chem.* 2010, **20**, 7682. (c) X-N. Li, Z-J. Wu, Z-J. Si, H-J. Zhang, L. Zhou. X-J. Liu, *Inorg. Chem*. 2009*,* **48**, 7740.
5. (a) P. J. Hay, W. R. Wadt, *J. Chem. Phys*. 1985, **82**, 270. (b) W. R. Wadt, P. J. Hay, J. Chem. Phys. 1985, **82**, 284. (c) P. J. Hay, W. R. Wadt, *J. Chem. Phys*. 1985, **82**, 299.
6. M. M. Francl, W. J. Pietro, W. J. Hehre, J. S. Binkley, M. S. Gordon, D. J. DeFrees, J. A. Pople, *J. Chem. Phys.,* 1982, **77**, 3654.
7. V. Barone, M. Cossi, *J. Phys. Chem. A,* 1998, **102**, 1995.
8. Frisch, M. J.; Trucks, G. W.; Schlegel, H. B.; Scuseria, G. E.; Robb, M. A.; Cheeseman, J. R.; Scalmani, G.; Barone, V.; Mennucci, B.; Petersson, G. A. et al. Gaussian 09, Revision D.01; Gaussian, Inc.: Wallingford, CT, 2009.
9. 8. S. Fantacci, F. D. Angelis and A. Selloni, J. Am. Chem. Soc., 2003, 125, 4381–4387.
10. D. D. Censo, S. Fantacci, F. D. Angelis, C. Klein, N. Evans, K. Kalyanasundaram, H. J. Bolink, M. Graetzel and M. K. Nazeeruddin, Inorg. Chem., 2008, 47, 980–989.
11. 10. R. L. Martin, J. Chem. Phys., 2003, 118, 4775–4777.